Mixed-species biofilms for high-cell-density application of *Synechocystis* sp. PCC 6803 in capillary reactors for continuous cyclohexane oxidation to cyclohexanol

Anna Hoschek,[#] Ingeborg Heuschkel,[#] Andreas Schmid, Bruno Bühler, Rohan Karande*,

Katja Bühler

[#]*both authors contributed equally to this manuscript*

Department of Solar Materials

Helmholtz-Centre for Environmental Research, UFZ

Permoserstrasse 15, 04318 Leipzig, Germany

* Corresponding author

Rohan Karande

Department of Solar Materials

Helmholtz-Centre for Environmental Research, UFZ

Permoserstrasse 15, 04318 Leipzig (Germany)

e-mail: rohan.karande@ufz.de

Phone: +49-341-235 48 22 71

Abstract

Photosynthetic microorganisms have enormous potential to produce fuels and value-added compounds sustainably. Efficient cultivation concepts that enable optimal light and CO_2 supply are necessary for the realization of high cell densities (HCDs), and subsequently for process implementation. We introduce capillary biofilm reactors with a high surface to volume ratio, and thus enhanced light availability, enabling HCDs of photo-autotrophic microorganisms. However, oxygenic photosynthesis leads to O_2 accumulation in such systems, impairing biofilm growth. We combined O_2 producing *Synechocystis* with O_2 respiring *Pseudomonas* using proto-cooperation to achieve HCDs of up to 51.8 g_{BDW} L^{-1}. This concept was coupled to the challenging C-H oxyfunctionalization of cyclohexane to cyclohexanol with a remarkable conversion of >98% and selectivity of 100 % (KA oil). High photoautotrophic biocatalyst concentrations were established and resulted in a productivity of 3.76 $g_{cyclohexanol}$ m^{-2} day^{-1}, which was maintained for at least one month.

Keywords

2

1. Introduction

In Nature, almost 385 billion tons of CO_2 are fixed annually to reduced organic materials by photosynthesis (Appel et al., 2013). This power of photosynthesis will be key to make inorganic carbon available for the production of value-added chemicals and fuels and reduce future dependency on fossil resources. Despite photo-catalysis developing remarkably and the huge potential of photoautotrophic microorganisms for eco-efficient production scenarios (Zhang et al., 2018), photo-biotechnology is still in its infancy. The lack of scalable photobioreactors that provide efficient light transmission, CO_2 supply, and O_2 degassing and thus enable high cell densities (HCD), constitutes a key bottleneck, especially if cost-sensitive bulk chemicals are the product of choice. Several reactor formats have been investigated on the laboratory scale, including tubular, flat, and column photobioreactors. Only tubular photobioreactors are operated on the industrial scale for the production of biomass or high priced chemicals (above 10€/kg). Examples include a 700 m^3 photobioreactor for the production of biomass for food and feed (Klötze, Germany) and a 25 m^3 photobioreactor for the production of astaxanthin (Hawaii, USA) (Fernandes et al., 2015).

Tubular photobioreactors with 100 to 600 mm inner diameter offer a surface area to volume ratio (SA/V) of over 100 $m^2\,m^{-3}$ enabling the efficient capturing of incident solar radiation (Posten, 2009). The high energy demand above 2000 W m^{-3} necessary for O_2 degassing and CO_2 supply constitutes a major disadvantage of such tubular reactors. It was estimated to excel the (chemical) energy harvested

3

from the sunlight (150 W m^{-3}) by a factor of 13-14 (Posten, 2009), prohibiting an economically feasible photo-biocatalytic production of lower-priced compounds. For enhancing light to chemical energy conversion efficiency, the tube diameter should be as small as possible. Capillary reactors with inner diameters of 0.5 to 3 mm are a promising option, due to an exceptionally high SA/V ratio of 1333-4000 $m^2\,m^{-3}$ and low light penetration depth (Posten, 2009), which may lead to an increase in the light to chemical energy conversion efficiency. Immobilization of the phototrophic organisms on such large surface area will allow maximal exploitation of the available light energy (Posten, 2009). Combining such an approach with biofilm cultivation adds advantages such as self-immobilization, self-regeneration, and high biomass retention within the reactor as compared to their suspended counterparts (Halan et al., 2012).

The capillary biofilm reactor concept has been applied for heterotrophic microorganisms utilizing carbohydrates as carbon, electron, and energy source, and recently has been adapted to the cultivation of the cyanobacterium *Synechocystis* sp. PCC 6803 (David et al., 2015). However, as a consequence of photosynthetic water oxidation, cultivation of photoautotrophic organisms at high cell densities in enclosed reactor setups quickly becomes hampered by the local O_2 accumulation in the system (Huang et al., 2017; Weissman et al., 1988). O_2 accumulation in closed photobioreactors is considered the main obstacle for the development of industrial-scale photobioreactors (Vonshak & Torzillo, 2013). Thus, the stable cultivation of photoautotrophic organisms at high cell densities in

4

capillary biofilm reactors necessitates *in situ* O_2 removal from the bulk aqueous phase.

Whereas technical approaches aim at the facilitated gas exchange with the environment (Weissman et al., 1988), we present a nature-inspired dual-species concept to relieve oxidative stress and enable the robust cultivation of HCD photoautotrophic biofilms in capillary bio-reactors (Fig. 1). Two microbial species with complementary properties regarding O_2 metabolism were co-cultivated as a biofilm in a capillary reactor: the O_2 evolving *Synechocystis* sp. PCC 6803 and the O_2 respiring *Pseudomonas taiwanensis* VLB120. Eventually, the resulting mixed-trophies biofilm setting enabled enhanced biomass formation compared to single-species biofilm settings. Furthermore, this dual-species HCD cultivation concept has been applied for continuous cyclohexane oxyfunctionalization combining recombinant, cyclohexane monooxygenase containing strains of *Synechocystis sp.* PCC 6803 and *Pseudomonas taiwanensis* VLB120.

2. Materials and methods

2.1. Chemicals. Chemicals used for medium preparation were purchased from Carl-Roth GmbH (Karlsruhe, Germany), Merck (Darmstadt, Germany), or Sigma-Aldrich (Steinheim, Germany) in the highest purity available. Cyclohexane, ≥ 99.8 % purity, was purchased from Merck (Darmstadt, Germany) and cyclohexanone and cyclohexanol, ≥ 99.5 % purity, were purchased from Sigma-Aldrich (Steinheim, Germany).

2.2. Bacterial strains and plasmids. Strains, plasmids, and primers used in this study are listed in the supplemental section (Heuschkel et al., 2019). Transformation with respective plasmids was performed by electroporation using kanamycin as the selection marker. Cloning procedures were based on standard methods (Sambrook & Russell, 2001).

2.3. Cultivation of *Synechocystis* sp. PCC 6803 strains. Cells were grown in YBG11 medium without citrate and supplemented with 50 mM $NaHCO_3$ (composition given in supplemental section). Pre-cultures were inoculated in 20 mL medium in a 100 mL baffled shake flask using 200 µL of a *Synechocystis* sp. PCC 6803 cryo-stock and incubated at 30 °C, 50 µE m^{-2} s^{-1} (LED), ambient CO_2 (0.04%), 150 rpm (2.5 cm amplitude), and 75% humidity in an orbital shaker (Multitron Pro shaker, Infors, Bottmingen, Switzerland) for 4 days. Pre-cultures were used to inoculate main cultures to an OD_{750} of 0.08. Main cultures were incubated for 4 days under the same conditions.

2.4. Cultivation of *Pseudomonas* sp. VLB120 strains. Overnight cultures were inoculated from a cryo-stock containing *Pseudomonas* sp. VLB120 using 5 mL LB medium and grown at 30 °C and 200 rpm (2.5 cm amplitude) in a Multitron Pro shaker (Infors). Minimal medium pre-cultures were inoculated by adding 200 µL of this overnight culture to 20 mL M9 medium (5 g L^{-1} citrate, US* trace elements) and incubated for 24 h (Emmerling et al., 2002). These pre-cultures were used to inoculate main cultures to an OD_{450} of 0.2. Main cultures were grown under the

6

same conditions for 8 h in 50 mL M9 medium (5 g L^{-1} citrate, US* trace elements) in 250 mL baffled shake flasks.

2.5. Pre-mixing of bacterial strains. Twenty mL of each main culture (*Synechocystis* sp. PCC 6803 and *Pseudomonas* sp.VLB120) were centrifuged (5000 g, RT, 7 min), washed in 20 mL and resuspended in 40 mL YBG11 medium (w/o citrate, 50 mM $NaHCO_3$). Ten mL of each of the two resulting cell suspensions with OD_{750} and OD_{450} values of 2.2 and 2.4, respectively, were mixed in a 100 mL baffled shake flask and incubated at 30 °C, 50 μmol m^{-2} s^{-1} (LED), ambient CO_2 (0.04%), 150 rpm (2.5 cm amplitude), and 75% humidity in a Multitron Pro shaker (Infors) for 24 h. Single species control cultures were composed of 10 mL cell suspension mixed with 10 mL of YBG11 medium (w/o citrate, 50 mM $NaHCO_3$).

2.6. Technical setting of the capillary reactor system. For biofilm cultivation, a capillary reactor system adapted from David et al. 2015 was applied (David et al., 2015). Serological pipettes functioned as capillaries for biofilm growth (trimmed to a capillary volume of 1.2 mL by cutting the tip and the intake area; inner diameter: 3 mm, length: 16.6 cm, Labsolute, Th. Geyer GmbH & Co. KG, Renningen, Germany). YBG11 medium (supplemented with 50 mM $NaHCO_3$, with or without 0.4 g L^{-1} citrate) was supplied via Tygon tubing (LMT-55, 2.06 mm inner diameter, 0.88 mm wall thickness; Ismatec, Wertheim, Germany) using a peristaltic pump (ISM939D; Ismatec). Air segments were supplied to the capillary reactor system via Tygon tubing connected by a T-connector. Injection ports (ibidi GmbH, Martinsried, Germany) were introduced in front of the capillaries for inoculation by

7

syringe. Fluorescence-light tubes were used as a light source (50 µmol m^{-2} s^{-1} measured at the center of the capillaries). Gas exchange at the medium inlet, for air segment generation, and at the medium outlet was enabled sterile trough filters (0.2 µm). Cultivation was performed at room temperature (RT, 22 to 26 °C).

2.7. Inoculation of the capillary reactor system. The capillaries of the reactor system were inoculated with single or mixed species suspensions by purging ca. 5 mL of each culture through the injection port. The medium flow was started 15 – 24 h after inoculation at a rate of ca. 52 µL min^{-1}. If indicated, air segments were introduced 9 days after inoculation at a rate of ca. 52 µL min^{-1}, resulting in an increased overall flow rate of ca. 104 µL min^{-1} in these capillaries.

2.8. O_2 quantification in gas and liquid phases. For O_2 quantification in air segments, bubble traps (sealed with a septum) were introduced downstream of capillaries and left 24 hours at least to equilibrate. Gas phase (100 µL) was sampled from the bubble trap using a gas-tight syringe (Hamilton, Reno, NV). O_2 was quantified using a Trace 1310 gas chromatograph (Thermo Fisher Scientific, Waltham, MA) equipped with a TG-BOND Msieve 5A capillary column (30 m, I.D.: 0.32 mm, film thickness: 30 µm, ThermoFisher Scientific) and a thermal conductivity detector operating at 100 °C with a filament temperature of 300 °C and a reference gas flow rate of 4 mL min^{-1}. Argon gas was applied as carrier gas at a constant flow rate of 5 mL min^{-1}. The injection temperature was set to 50 °C and a split ratio of 2 was applied. The oven temperature was kept constant at 35 °C for 3 min. O_2 concentrations in the liquid medium were quantified using a Clark-type

flow-through sensor (OX-500 Oxygen Microsensor, Unisense, Aarhus, Denmark) equipped with a microsensor amplifier (Microsensor multimeter, Unisense).

2.9. Citrate quantification. Samples were collected from the capillary outlet, centrifuged (17000g, 5 min, RT), and the supernatant was applied for high-pressure liquid chromatography (Dionex Ultimate 300, Thermo Fisher Scientific) equipped with a ligand exchange column (HyperREZ XP Carbohydrate H+, 30 cm length, 7.7 mm diameter, 8 μm particle size, ThermoFisher Scientific) and a variable wavelength detector operating 210 nm. The column oven temperature was kept constant at 40 °C. 16 mM H_2SO_4 was applied as carrier solvent at a flow rate of 0.75 mL min^{-1}.

2.10. Biotransformation of cyclohexane in capillary biofilm reactors.
Heterologous expression of cytochrome P450 cyclohexane monooxygenase genes in *P. taiwanensis* VLB120_pAH050 (in short *Ps*_CYP) and/or *Synechocystis* sp. PCC 6803_ pAH050 (in short *Syn*_CYP) was induced after 36 days of cultivation by adding 2 mM IPTG to the medium feed. At day 37, a cyclohexane feed was connected to the capillary reactor to start the biotransformation. For constant cyclohexane supply, the segmented medium and air feed was channeled through a silicon tube of 20 cm length inserted into a closed 100 mL Schott glass bottle containing 80 mL cyclohexane. The cyclohexane permeability of the silicone tube enabled efficient and constant diffusion of cyclohexane into the medium-air feed. The high cyclohexane vapor pressure (121.721 mm Hg at 30°C, Henry's law constant $K_{air/water}$ 0.15 atm m^3 $mole^{-1}$) and very low water solubility (55 mg L^{-1}) result

into a higher amount of cyclohexane in the gas phase as compared to the aqueous phase. The total inlet cyclohexane concentration was ca. 1 mM.

2.11. Quantification of cyclohexanol and cyclohexanone using gas chromatography (GC). Reactor samples (1.2 ml) were collected from the outlet and inlet of the capillaries. One mL of the liquid phase samples was extracted with 500 µL of ice-cold diethyl ether (containing 0.2 mM decane added as internal standard) by vigorous mixing for 2 min followed by centrifugation (17,000xg, 2 min, RT). The ether phase was removed and dried over anhydrous Na_2SO_4. Cyclohexanol in the ether phase then was quantified using a GC Trace 1310 (Thermo Fisher Scientific) equipped with a TG-5MS capillary column (5% diphenyl / 95% dimethyl polysiloxane, 30 m, I.D., 0.25 mm, film thickness: 0.25 µm, Thermo Fisher Scientific) and a flame ionization detector operated at 320 °C, 350 mL min^{-1} air, 30 mL min^{-1} makeup gas, and 35 mL min^{-1} hydrogen gas flow rates. N_2 was applied as carrier gas at a constant flow of 1.5 mL min^{-1}. An injection volume of 1 µL sample was performed using a PTV injector, programmed with a temperature gradient of 10 °C s^{-1} from 90-300 °C. A split ratio of 11 was applied. Oven temperature profile applied was as follows: 40 °C for 1 min, 40-80 °C at 10 °C min^{-1}, 80-320 °C at 100 °C min^{-1}, and 320 °C for 10 min.

2.12. Determination of cell number, cell volume, and biofilm dry weight. For respective quantifications, the capillary reactor set-up was disassembled. The biomass was removed from the capillary reactor by scratching the inner wall of the capillary with a 120 mm long hypodermic-needle and rinsing these parts thoroughly

10

with water to remove detached biomass. The recovered biomass was suspended in 20 mL of water and mixed vigorously for 1 min, before cell number, and cell volume was quantified using a Coulter counter (Multisizer 3, 20 μm aperture, Beckman Coulter, Brea, CA). *Synechocystis* sp. PCC 6803 and *P. taiwanensis* VLB120 cells were differentiated via their size applying a range of 0.4 - 1.6 μm and 1.6 – 6 μm, respectively. For biofilm dry weight determination, the total biomass was concentrated by centrifugation (5000g, 20 °C, 7 min), transferred to pre-dried and pre-weighed glass tubes, centrifuged again (5000g, 4 °C, 7 min), and the resulting pellet dried at 60 °C for 1 week before the final weighing was performed.

2.13. CLSM imaging of the mixed trophies biofilm. For confocal microscopic imaging, *Synechocystis* sp. PCC 6803 and *P. taiwanensis* VLB120_egfp were used for biofilm cultivations in a custom-made flow cell (dimensions: length 65 mm, height 3 mm, width 4.5 mm; Heuschkel et al., 2019). Preparation of (pre-) cultures and mixed species suspensions was performed as described above. The flow cell was flushed for 2 h with YBG11 medium and inoculated with 2 mL cell suspension. After 24 h, the medium flow was started (52 μL min^{-1}) and the biofilm was grown for 10 days. Next, the air flow was started at 52 μL min^{-1}. A Zeiss LSM 710 NLO confocal laser microscope (Jena, Germany) equipped with a 488 nm and a 633 nm laser line for the excitation of eGFP and cyanobacterial autofluorescence, respectively, was used for image acquisition. Stacks of images with single-cell resolution were taken with an LD C-Apochromat 40x/1.1 W objective. 3D image reconstruction was performed with IMARIS (Bitplane AG, Zurich, Switzerland).

11

3. Results and discussion

In nature, oxygenic phototrophs and aerobic heterotrophs are embedded in a complex matrix of extracellular polymeric substances (EPS) to form stable microbial mats (Prieto-Barajas et al., 2017). In such mats, the microbial consortium interacts in close cooperation and thereby profits from complementary metabolic activities. In wastewater treatment plants, undefined microalgal / cyanobacterial biofilm consortia are applied for, e.g., effluent oxygenation, heavy metal removal, and recycling of nitrogen and phosphor (Barros et al., 2018). Some decades ago, Nature-based concept based on *in-situ* O_2 supply had been adapted for productive biocatalysis by utilizing defined co-cultures of algae and bacteria (Adlercreutz et al., 1982; Adlercreutz & Mattiasson, 1982). Respective research either focused on immobilized cells embedded in a polymeric matrix such as alginate or on cell suspensions. Our study takes up the concept of such microbial cooperation, translating it into a defined and minimized biofilm system profiting from cooperative stabilization.

In order to evaluate if a photoautotrophic-chemoheterotrophic dual-species concept allows the establishment of stable phototrophic HCD biofilms, we co-cultivated the two model strains *Synechocystis* sp. PCC 6803 and *P. taiwanensis* VLB120 in a capillary reactor system. *Synechocystis* sp. PCC 6803 is a well-known cyanobacterial workhorse widely used for studying photosynthesis-driven production of value-added chemicals and fuels (Nozzi et al., 2013). *P. taiwanensis* VLB120 constitutes a chemoheterotrophic strain frequently applied for biocatalytic

purposes with strong biofilm formation ability (Gross et al., 2010). Both strains carried the empty expression plasmid pAH032 containing a kanamycin resistance cassette. After 5 weeks of biofilm maturation in the capillary reactor, O_2 concentrations in the liquid and gas phases as well as citrate consumption (when applicable) were quantified, followed by biomass analysis in terms of photo-pigment content (macroscopic), bio-volume of each species (cell number and cell volume), and total biofilm dry weight. Six independent cultures were investigated, comprising single-species *Synechocystis* sp. PCC 6803 biofilms and dual-species mixed trophies biofilms. First, results obtained from monoseptic cultivation in organic carbon free YBG11 medium are presented, followed by dual-species in the same medium. Finally, dual-species cultivation in YBG11 medium supplemented with citrate as an organic source of carbon and energy is shown.

3.1. Surface coverage and biofilm development in the capillary reactor are impaired in phototrophic single-species biofilms. As a reference, *Synechocystis* sp. PCC 6803 (pAH032) was grown monoseptically in the capillary reactor. Without the provision of air segments (mere aqueous feed), biofilm growth was very weak (Fig. 2i) and resulted in a high O_2 concentration at the outlet (746 µM, Fig. 3i). The biofilm color turned from green to yellowish towards the end of the tubing indicating impaired cell viability and photosynthesis. High O_2 concentrations may promote the formation of radical oxygen species (ROS) as a side product of oxygenic photosynthesis. The impact of ROS on photoautotrophic organisms and the strategies these organisms have developed to cope with oxygen stress are

13

investigated since long (Fahey, 2013). However, studies investigating the influence of elevated O_2 levels on growth physiology of cyanobacteria are scarce. ROS formation is promoted when the intensity of light-driven electron transport outpaces the rate of electron consumption during CO_2 fixation resulting in damage of photosystem II and associated photo-pigments (Latifi et al., 2009). This might be reflected by the yellowish color of the cells observed in the experiments with high O_2 (Fig. 2 i/iii).

The introduction of air segments into the medium flow had a positive effect on biofilm growth and fitness, as can be concluded from the dense, green colored biofilm and the final biomass concentrations, which increased from 2 to 14 g_{BDW} L^{-1} (Fig. 2ii). The air segments led to oxygen extraction and reduced the aqueous O_2 concentration at the outlet (284 µM, Fig. 3ii). However, the biofilm was only loosely attached, and surface coverage was inhomogeneous.

3.2. Phototrophic biofilm growth in capillary reactors profits from the dual-species mixed trophies concept. In order to evaluate the hypothesized benefits of a dual-species mixed trophies approach, i.e., improved biofilm attachment and reduced O_2 stress, *Synechocystis* sp. PCC 6803 (pAH032) and *P. taiwanensis* VLB120 (pAH032) were inoculated in capillary reactors at a ratio of 1:1. As described above for single-strain biofilms, cultivations were performed under either aqueous or aqueous-air segmented flow conditions.

Compared to the monoseptic cultures described above, the biofilm dry weight after 5 weeks increased by a factor of three and two under, aqueous and aqueous-air

14

segmented flow conditions, respectively (Fig. 2 iii/iv). As no organic carbon source was supplied via the medium feed, extracellular (polymeric) substances from *Synechocystis* and/or compounds originating from cell lysis constituted the only carbon and energy source for *P. taiwanensis.* Thus, *Pseudomonas* cells only represented a minor fraction of the total biomass (Fig. 3iii/iv). Under aqueous flow conditions, very high O_2 concentrations (923 µM) were reached, which can be attributed to the low availability of organic carbon and energy sources functioning as electron sources for respiration of *Pseudomonas.* Despite of the higher biomass, biofilm coverage was poor, and, towards the end of the capillary, cells showed a yellowish color. In contrast, the introduction of air segments facilitated O_2 extraction and, in combination with the presence of the O_2 respiring strain, resulted in a high phototrophic cell density (31 $g_{BDW}L^{-1}$) and complete surface coverage at 287 µM oxygen. In summary, the presence of *Pseudomonas* cells promoted *Synechocystis* biofilm growth and was essential to achieve 100% surface coverage, when O_2 was extracted using air segments.

3.3. Citrate addition relieves oxidative stress and supports HCD cultivation of *Synechocystis* sp. PCC 6803. Based on the hypothesis that increased respiratory activity and biomass fraction of *Pseudomonas* cells may further support phototrophic biofilm formation, the YBG11 medium fed to the capillary reactor was supplemented with 0.4 g L^{-1} citrate. Again, an equal mixture of the two strains was used for the inoculation of capillary reactor setups, which then were operated for 5 weeks either in mere aqueous or aqueous-air segmented flow mode.

15

Without air segments, citrate catabolism coupled to O_2 respiration decreased the O_2 concentration in the aqueous phase to anoxic levels (Fig. 3v). This together with an increased *Pseudomonas* biomass fraction, promoted cyanobacterial biofilm formation as it is reflected by the 48 g_{BDW} L^{-1} biofilm dry weight (85% cyanobacterial cells). Surprisingly, the addition of air segments reduced the final biofilm dry weight to 19 g_{BDW} L^{-1} (Fig. 2vi). This and the reduced *Pseudomonas* biomass fraction (8%, Fig. 3vi) indicate a detrimental effect of the air segments on the biofilm growth of *P. taiwanensis* VLB120.

It remains puzzling why only poor biomass development occurred when segmented flow was combined with favorable growth conditions for *Pseudomonas* (citrate supply, Fig. 2 vi). The high citrate consumption at low biomass concentrations (0.39 g L^{-1} compared to 0.27 g L^{-1} without air segments) may reflect a hydrodynamic stress response of *Pseudomonas*, induced by the hydrodynamic forces imposed onto the microbes via the air segments. Elevated energy demand and thus catabolism is well described for stress response mechanisms (Nicolaou et al., 2010). Microbial stress response has been a matter of detailed investigation since long, although mainly in the context of solvent tolerance, where energy-dependent processes such as the employment of efflux pumps and heat shock proteins are directly entangled with the energy metabolism. Regarding hydrodynamic stress, studies mostly focused on the biofilm attachment/detachment processes and the effect of shear forces on biofilm architecture (Karimi et al., 2015). In this context, it appears likely that energy demanding mechanisms also

16

affect *Pseudomonas* biomass development in the capillary reactors under segmented flow conditions. In summary, the dual-species mixed trophies approach enabled the cultivation of photobiocatalysts in a stable and high cell density format, thereby overcoming a key-bottleneck in photo-biotechnology.

3.4. *Pseudomonas* cells promote phototrophic HCD biofilm cultivation by surface conditioning and O$_2$ removal. The influence of *Pseudomonas* cells on the development of phototrophic biofilm was further investigated using confocal laser scanning microscopy (CLSM) (Fig. 4). Biofilm growth and development of the mixed species was studied over 25 days using a custom-designed microscopy flow cell (Heuschkel et al., 2019).

After inoculation, both strains settled on the capillary surface in close vicinity to each other with *Pseudomonas* forming a kind of cell layer on the attachment surface (Fig. 4; first panel). In the course of cultivation, *Synechocystis* was observed to overgrow the *Pseudomonas* layer slowly. The start of aqueous-air segmented flow after 10 days did not cause any biofilm detachment, which indicates strong adhesion of the organisms resisting the fluidic and interfacial forces. It is remarkable that the biomass was not flushed out of the system upon the introduction of air segments, as it is reported for monoseptic *Pseudomonas* biofilms (Karande et al., 2014).

Overall, CLSM analysis reveals that the two strains grew in close vicinity to each other during the initial phase of biofilm formation and that *Synechocystis* was overgrowing this layer at a later stage of biofilm maturation (Fig. 4). These results

17

indicate that proto-cooperation between the two strains actively facilitates surface attachment of both strains as also discussed in Nadell et al., (Nadell et al., 2016). However, comparing capillary reactor and flow cell experiments one needs to keep in mind, that the flow cell used for the microscopic analysis was composed of different materials (glass and stainless steel) then the capillary reactor (plastic), which could influence attachment behavior.

3.5. Mixed trophies biofilms are potent photoautotrophic biocatalysts. To exemplify the application benefit of the dual-species mixed trophies biofilm approach, we evaluated biocatalytic cyclohexane oxyfunctionalization to cyclohexanol. Cyclohexane oxidation is of central interest for Nylon 6 and Nylon 66 production. However, the activation of chemically inert C-H bonds in hydrocarbons is inherently difficult making specific catalytic C-H oxidation one of the "dream reactions" from chemical and industrial perspectives {Roduner, 2013 #23}. The hydroxylation of C-H bonds in cyclohexane has an industrial history of more than 70 years, but several vital challenges persist (Schuchardt et al., 2001). Low cyclohexane conversion (~6%) and combinatorial selectivity of 80-90% (cyclohexanol and cyclohexanone) due to multiple oxidations, as well as safety issues resulting from harsh operating conditions still challenge chemical cyclohexane conversion (Fischer et al., 2010). Alternative chemical processes are evaluated, but controlling selectivity at high conversion remains problematic (Schuchardt et al., 2001).

The development of biological routes for cyclohexane oxidation process is difficult since cyclohexane is highly toxic for microorganisms and somewhat challenging to handle due to its physicochemical properties. To the best of our knowledge, there is only one example reported so far, employing a heterotrophic organism for continuous conversion of cyclohexane oxidation to cyclohexanol (Karande et al., 2016). The necessary supply of organic compounds functioning as electron donors constitutes a drawback of these concepts and has been identified as the main cost driver for the synthesis of low price bulk chemicals (Kuhn et al., 2010; Mathys et al., 1999). To overcome this issue, we exploited *Synechocystis* sp. PCC6803 as a photoautotrophic workhorse utilizing water as electron (and O_2) source for C-H hydroxylation and CO_2 as a carbon source for biomass formation (Hoschek et al., 2017).

Cyclohexane monooxygenase encoding genes were introduced into *Synechocystis* sp. PCC 6803 and *P. taiwanensis* VLB120 using pAH050 yielding *Syn*_CYP and *Ps*_CYP, respectively. Both recombinants were mixed in a ratio of 1:1 and used to inoculate capillary reactors as described before. Cyclohexane oxidation was evaluated under the dual-species mixed trophies conditions used above in setup iv (Fig. 2), i.e., with the supply of air segments and without citrate provision. After 5 weeks of cultivation, the biotransformation was started by the addition of the biotransformation substrate cyclohexane to the aqueous-air segmented feed flow.

After 1 day of adaptation to the biotransformation conditions, the biofilm reached its maximal cyclohexanol production rate of 3.76 g_{CHXOH} m^{-2} day^{-1} (Fig. 5; Heuschkel

19

et al., 2019). Cyclohexanol (CHXOH) constituted the main product and was accompanied by low amounts of the overoxidation product cyclohexanone as the only byproduct. During the following days, the product formation rate was constant. The light was switched off to investigate the dependency of the heterologous reaction on photosynthesis on days 8 and 10. The biocatalytic system responded by a significant reduction of the biotransformation rate to 1.0-1.3 g_{CHXOH} m^{-2} day^{-1}. These results clearly show that mainly *Synechocystis* was responsible for the biotransformation activity and that photosynthetic water oxidation served as the primary source of the electrons necessary to drive the oxyfunctionalization reaction. Possibly, storage compounds were mobilized and thus fueled the reaction also under dark conditions.

The system exhibited remarkable stability remaining active for a month before the experiment was actively terminated. This photobiocatalytic process reached very high values for cyclohexane conversion (98.9%) and reaction selectivity (84.5% cyclohexanol and 15.5% cyclohexanone; averaged over the complete operation period). O_2 balancing without and with biotransformation revealed that 50% of the O_2 produced via photosynthetic water oxidation was utilized in the biocatalytic reaction. These results highlight the enormous potential of the dual-species mixed trophies concept and particular HCD phototrophic biofilms for efficient and stable biocatalytic oxyfunctionalization.

The successful photobiocatalytic biotransformation of cyclohexane to cyclohexanol demonstrated the basic feasibility of such an approach for biotechnological

application. Overall, dual-species phototrophic biofilms enabled continuous cyclohexane oxidation for at least a month with volumetric productivity of 0.2 g L^{-1}h^{-1}. This is about half of the performance achieved when applying monoseptic *P. taiwanensis* VLB120 for which a space-time-yield of 0.4 g L^{-1} h^{-1} is reported (Karande et al., 2016). However, it is important to note, that this was only achieved, when the biotransformation was conducted in complex medium. The biological system achieved a remarkable cyclohexane conversion of 98% and a selectivity of 100%, compared to 6% and 80-90%, respectively, for the chemical process (Fischer et al., 2010). Insufficient was the current space-time-yield being about 125 fold lower than of the chemical process. However, it needs to be taken into account that this is the first proof of concept study with no reaction or catalyst optimization being done yet.

This continuous HCD biofilm reactor concept can be transferred to other phototrophic biocatalytic systems reported in literature such as alkane monooxygenase-,(Hoschek et al., 2017) Baeyer–Villiger monooxygenase-,(Böhmer et al., 2017) or enoate reductase-based systems (Köninger et al., 2016). On the other hand, it may also solve the severe problem of O$_2$ limitation in productive, heterotrophic biofilms. Continuous production of chemicals using *P. taiwanensis* VLB120 in capillary biofilm reactors already has been investigated in several studies (Gross et al., 2010). As for many O$_2$-dependent bioprocesses, O$_2$ mass transfer constituted the main process limitation (Karande et al., 2014). Here, the

coupling of photosynthetic O_2 generation with aerobic heterotrophic metabolism extends the scope of O_2-dependent bioprocesses (Hoschek et al., 2018).

This concept now awaits further optimization and implementation for the eco-efficient production of chemicals (Sheldon & Woodley, 2018). For chemical processes microreactors are already implemented at larger scale based on the numbering-up approach (Al-Rawashdeh et al., 2012; Hessel, 2005). For our concept a similar approach would be followed. However, challenges concerning light distribution and material costs need to be solved. It has a vast potential to circumvent previous fundamental limitations of today´s photobioreactors. Next, to biocatalytic applications like complex cascade reactions (Zhou et al., 2015), mixed-trophies biofilms could be a valuable tool for other research fields, such as bioremediation, ecotoxicology, or biophotovoltaics (Wenzel et al., 2018).

4. Conclusions

This work demonstrates prototrophy as a biological strategy for the cultivation of photobiocatalysts in a stable and high cell density format up to 51.8 g_{BDW} L^{-1}, thereby overcoming a key-bottleneck in photo-biotechnology. The crucial problem of O_2 accumulation and thus toxification/inhibition of the photoautotrophic biocatalyst in capillary reactor was overcome by utilizing O_2 respiring *P. taiwanensis* VLB120, O_2 extracting air segments and by O_2 dependent biotransformation. Mixed trophies biofilms in capillary reactors were able to produce 3.76 g m^{-2} day^{-1} cyclohexanol for over a month with conversion, and KA oil

selectivity values of 98% and 100%, respectively, a milestone in cyclohexane-based chemistry.

5. Acknowledgments

6. References

1. Adlercreutz, P., Holst, O., Mattiasson, B. 1982. Oxygen-Supply to Immobilized Cells .2. Studies on a Coimmobilized Algae-Bacteria Preparation with Insitu Oxygen Generation. *Enzyme and Microbial Technology*, **4**(6), 395-400.
2. Adlercreutz, P., Mattiasson, B. 1982. Oxygen-Supply to Immobilized Cells .3. Oxygen-Supply by Hemoglobin or Emulsions of Perfluorochemicals. *European Journal of Applied Microbiology and Biotechnology*, **16**(4), 165-170.
3. Al-Rawashdeh, M., Yu, F., Nijhuis, T.A., Rebrov, E.V., Hessel, V., Schouten, J.C. 2012. Numbered-up gas-liquid micro/milli channels reactor with modular flow distributor. *Chemical Engineering Journal*, **207**, 645-655.
4. Appel, A.M., Bercaw, J.E., Bocarsly, A.B., Dobbek, H., DuBois, D.L., Dupuis, M., Ferry, J.G., Fujita, E., Hille, R., Kenis, P.J.A., Kerfeld, C.A., Morris, R.H., Peden, C.H.F., Portis, A.R., Ragsdale, S.W., Rauchfuss, T.B., Reek, J.N.H., Seefeldt, L.C., Thauer, R.K., Waldrop, G.L. 2013. Frontiers, opportunities, and challenges in biochemical and chemical catalysis of CO_2 fixation. *Chemical Reviews*, **113**(8), 6621-6658.
5. Barros, A.C., Gonçalves, A.L., Simões, M. 2018. Microalgal/cyanobacterial biofilm formation on selected surfaces: the effects of surface physicochemical properties and culture media composition. *Journal of Applied Phycology*, **https://doi.org/10.1007/s10811-018-1582-3**.
6. Böhmer, S., Köninger, K., Gómez-Baraibar, Á., Bojarra, S., Mügge, C., Schmidt, S., Nowaczyk, M.M., Kourist, R. 2017. Enzymatic oxyfunctionalization driven by photosynthetic water-splitting in the cyanobacterium *Synechocystis* sp. PCC 6803. *Catalysts*, **7**(8), 240-248.
7. David, C., Bühler, K., Schmid, A. 2015. Stabilization of single species *Synechocystis* biofilms by cultivation under segmented flow. *Journal of Industrial Microbiology and Biotechnology*, **42**(7), 1083-1090.
8. Emmerling, M., Dauner, M., Ponti, A., Fiaux, J., Hochuli, M., Szyperski, T., Wüthrich, K., Bailey, J., Sauer, U. 2002. Metabolic flux responses to pyruvate kinase knockout in *Escherichia coli. Journal of bacteriology*, **184**(1), 152-164.
9. Fahey, R.C. 2013. Glutathione analogs in prokaryotes. *Biochimica et Biophysica Acta (BBA) - General Subjects*, **1830**(5), 3182-3198.
10. Fernandes, B.D., Mota, A., Teixeira, J.A., Vicente, A.A. 2015. Continuous cultivation of photosynthetic microorganisms: Approaches, applications and future trends. *Biotechnology Advances*, **33**, 1228-1245.
11. Fischer, J., Lange, T., Boehling, R., Rehfinger, A., Klemm, E. 2010. Uncatalyzed selective oxidation of liquid cyclohexane with air in a microcapillary reactor. *Chemical Engineering Sciencees*, **65**, 4866-4872.
12. Gross, R., Lang, K., Bühler, K., Schmid, A. 2010. Characterization of a biofilm membrane reactor and its prospects for fine chemical synthesis. *Biotechnology and Bioengineering*, **105**(4), 705-717.
13. Halan, B., Buehler, K., Schmid, A. 2012. Biofilms as living catalysts in continuous chemical syntheses. *Trends in Biotechnology*, **30**(9), 453-465.
14. Hessel, V. 2005. From microreactor design to microreactor process design. *Chemical Engineering & Technology*, **28**(3), 243-243.

15. Heuschkel, I., Hoschek, A., Schmid, A., Bühler, B., Karande, R., Bühler, K. 2019. Data on mixed trophies biofilm for continuous cyclohexane oxidation to cyclohexanol using Synechocystis sp. PCC 6803. *Data in Brief*.

16. Hoschek, A., Bühler, B., Schmid, A. 2017. Overcoming the gas–liquid mass transfer of oxygen by coupling photosynthetic water oxidation with biocatalytic oxyfunctionalization. *Angewandte Chemie International Edition*, **56**(47), 15146-15149.

17. Hoschek, A., Schmid, A., Bühler, B. 2018. *In situ* O$_2$ generation for biocatalytic oxyfunctionalization reactions. *ChemCatChem*, **10**(23), 5366-5371.

18. Huang, Q., Jiang, F., Wang, L., Yang, C. 2017. Design of photobioreactors for mass cultivation of photosynthetic organisms. *Engineering*, **3**(3), 318-329.

19. Karande, R., Debor, L., Salamanca, D., Bogdahn, F., Engesser, K.H., Buehler, K., Schmid, A. 2016. Continuous cyclohexane oxidation to cyclohexanol using a novel cytochrome P450 monooxygenase from *Acidovorax* sp. CHX100 in recombinant *P. taiwanensis* VLB120 biofilms. *Biotechnology and Bioengineering*, **113**(1), 52-61.

20. Karande, R., Halan, B., Schmid, A., Buehler, K. 2014. Segmented flow is controlling growth of catalytic biofilms in continuous multiphase microreactors. *Biotechnology and Bioengineering*, **111**(9), 1831-1840.

21. Karimi, A., Karig, D., Kumar, A., Ardekani, A.M. 2015. Interplay of physical mechanisms and biofilm processes: review of microfluidic methods. *Lab Chip*, **15**(1), 23-42.

22. Köninger, K., Gómez Baraibar, Á., Mügge, C., Paul, C.E., Hollmann, F., Nowaczyk, M.M., Kourist, R. 2016. Recombinant cyanobacteria for the asymmetric reduction of C=C bonds fueled by the biocatalytic oxidation of water. *Angewandte Chemie International Edition*, **55**(18), 5582-5585.

23. Kuhn, D., Kholiq, M.A., Heinzle, E., Bühler, B., Schmid, A. 2010. Intensification and economic and ecological assessment of a biocatalytic oxyfunctionalization process. *Green Chemistry*, **12**(5), 815-827.

24. Latifi, A., Ruiz, M., Zhang, C.-C. 2009. Oxidative stress in cyanobacteria. *FEMS Microbiology Reviews*, **33**(2), 258-278.

25. Mathys, R.G., Schmid, A., Witholt, B. 1999. Integrated two-liquid phase bioconversion and product-recovery processes for the oxidation of alkanes: Process design and economic evaluation. *Biotechnology and Bioengineering*, **64**(4), 459-477.

26. Nadell, C.D., Drescher, K., Foster, K.R. 2016. Spatial structure, cooperation and competition in biofilms. *Nature Reviews Microbiology*, **14**, 589–600.

27. Nicolaou, S.A., Gaida, S.M., Papoutsakis, E.T. 2010. A comparative view of metabolite and substrate stress and tolerance in microbial bioprocessing: From biofuels and chemicals, to biocatalysis and bioremediation. *Metabolic engineering*, **12**(4), 307-331.

28. Nozzi, N., Oliver, J., Atsumi, S. 2013. Cyanobacteria as a platform for biofuel production. *Frontiers in bioengineering and biotechnology*, **1**, 7.

29. Posten, C. 2009. Design principles of photo-bioreactors for cultivation of microalgae. *Engineering in life sciences*, **9**(3), 165-177.

30. Prieto-Barajas, C.M., Valencia-Cantero, E., Santoyo, G. 2017. Microbial mat ecosystems: Structure types, functional diversity, and biotechnological application. *Electronic Journal of Biotechnology*, **31**, 48-56.

31. Sambrook, J., Russell, D. 2001. Molecular cloning - a laboratory manual. *Cold Spring Habour Laboratory Press, New York*.

32. Schuchardt, U., Cardoso, D., Sercheli, R., Pereira, R., de Cruz, R.S., Guerreiro, M.C., Mandelli, D., Spinace, E.V., Fires, E.L. 2001. Cyclohexane oxidation continues to be a challenge. *Applied Catalysis a-General*, **211**(1), 1-17.

33. Sheldon, R.A., Woodley, J.M. 2018. Role of Biocatalysis in Sustainable Chemistry. *Chemical Reviews*, **118**(2), 801-838.

34. Vonshak, A., Torzillo, G. 2013. Environmental Stress Physiology in: *Handbook of Microalgal Culture* (Eds.) Amos Richmond, Q. Hu, Whiley Blackwell.

35. Weissman, J.C., Goebel, R.P., Benemann, J.R. 1988. Photobioreactor design: mixing, carbon utilization, and oxygen accumulation. *Biotechnology and Bioengineering*, **31**(4), 336-344.

36. Wenzel, T., Härtter, D., Bombelli, P., Howe, C.J., Steiner, U. 2018. Porous translucent electrodes enhance current generation from photosynthetic biofilms. *Nature Communications*, **9**(1), 1299.

37. Zhang, W., Fernández-Fueyo, E., Ni, Y., van Schie, M., Gacs, J., Renirie, R., Wever, R., Mutti, F.G., Rother, D., Alcalde, M., Hollmann, F. 2018. Selective aerobic oxidation reactions using a combination of photocatalytic water oxidation and enzymatic oxyfunctionalizations. *Nature Catalysis*, **1**(1), 55-62.

38. Zhou, K., Qiao, K., Edgar, S., Stephanopoulos, G. 2015. Distributing a metabolic pathway among a microbial consortium enhances production of natural products. *Nature Biotechnology*, **33**, 377–383.

Figure captions

Fig. 1 Dual-species HCD biofilm cultivation in a capillary reactor. A photoautotrophic strain (here *Synechocystis* sp. PCC 6803; green cell) producing O_2 is cultivated together with a heterotrophic microbe (here *P. taiwanensis* VLB120; brown cell) as a biofilm in a capillary reactor. Growth medium is continuously running through the capillary. The system can be operated either under mere aqueous flow (Panel A) or under segmented flow (Panel B), where air segments are pumped through the system. For HCD cultivation it is crucial, that the oxygen concentration in the system is low. This oxygen removal can be achieved either via respiration using proto-cooperation, the introduction of an O_2 dependent reaction or by extraction of O_2 into air segments flowing through the capillary reactor.

Fig. 2 Images of the biofilm capillary reactors 5 weeks after inoculation. i) and ii) depict monoseptic biofilm cultures of *Synechocystis* sp. PCC 6803 (pAH032) (Syn_Km) without and with air segments, respectively. Dual species biofilm cultures of Syn_Km and *P. taiwanensis* VLB120 (pAH032) were inoculated at a ratio of 1:1 and operated iii) without and iv) with air segments. v) and vi) correspond to iii) and iv) with citrate in the aqueous medium feed. Final biomass concentrations are given on the right of the respective image. Aqueous medium was fed at a rate of 52 μL min^{-1}. For segmented flow, a gaseous air phase was additionally fed at the same rate. BDW, biomass dry weight.

Fig. 3 O_2 and final biomass concentrations of single- and dual-species biofilms grown in capillary biofilm reactors after 5 weeks of cultivation. Grey bars refer to the aqueous O_2 concentrations measured at reactor outlets (left axis). Filled bars refer to the biomass dry weight per capillary volume ($g_{BDW}L^{-1}$, right axis). The green part of the filled bars corresponds to the *Synechocystis* sp. fraction and the blue one to the respective *Pseudomonas* fraction. The black line indicates O_2 saturation under ambient conditions (1

27

atm; 25 °C). Indices given on the x-axis refer to the different cultivation settings as defined in the legend of Figure 2. BDW, biomass dry weight

Fig. 4 3D Reconstruction of CLSM images showing the growth of a dual-species mixed trophies biofilm under aqueous as well as aqueous-air segmented flow conditions. Green and red cells correspond to *P. taiwanensis* VLB120 with a green fluorescent protein encoding *egfp* gene integrated into its genome and *Synechocystis* sp. PCC 6803 with its chlorophyll an autofluorescence, respectively (eGFP: 488 nm laser line, 4.0% laser intensity, 620 detector gain, chlorophyll autofluorescence: 633 nm laser line, 1.0% laser intensity, 500 detector gain). The biofilm was cultivated in YBG11 medium at 22 °C. All images were reconstructed and analyzed using IMARIS (8.2.0). Quantitative data are given in Heuschkel et al., 2019.

Fig. 5 Biocatalytic cyclohexane oxyfunctionalization utilizing recombinant *Synechechocystis sp.* PCC 6803 (pAH050) and *P. taiwanensis* VLB 120 (pAH050) in a dual-species mixed trophies biofilm. Biotransformation (started day 0 in Fig. 5) was initiated after 5 weeks of biofilm cultivation. Experiments have been conducted at RT and 50 µE m^{-2} s^{-1} providing organic carbon free YBG11 medium and air segments at a flow rate of 52 µL min^{-1}. The light was switched off during days 8 and 10 for 24 hours, respectively. Green and gray bars represent product formation under light and dark conditions, respectively. Light and dark colors refer to the formation of cyclohexanol and cyclohexanone, respectively. (Further information are given in the supplemental section, see Heuschkel et al., 2019)

Table

Table 1 Cultivation and biotransformation parameters in the dual-species capillary reactor in the presence and absence of cyclohexane conversion.

Acc. O_2[1] (mM)	CHXOL (mM)	Total O_2 formed[2] (mM)	O_2 acc. rate (g m^{-2} day^{-1})	CHXOL formation rate (g m^{-2} day^{-1})	Conversion (%)	Selectivity (%)	Biomass (g$_{BDW}$/L)
Biotransformation condition[3]							
0.87 (± 0.24)	0.99 (± 0.08)	1.96 (± 0.34)	0.55 (± 0.15)	3.76 (± 0.31)	98.9	84.5 (100)[4]	51.8 (±3 .15)
Standard condition (no biotransformation)							
1.83 (± 0.36)	NA	2.00 (± 0.36)	1.15 (± 0.34)	NA	NA	NA	41.8 (± 1.50)

Acc = accumulation; CHXOL = Cyclohexanol; NA = not applicable.

[1] O_2 accumulation between the inlet and outlet of capillary reactors.

[2] Sum of accumulated O_2 and O_2 consumed for cyclohexane hydroxylation.

[3] As given in Fig.5

[4] Selectivity for cyclohexanol and cyclohexanone formation, as usually described for chemical processes.(Fischer et al., 2010)
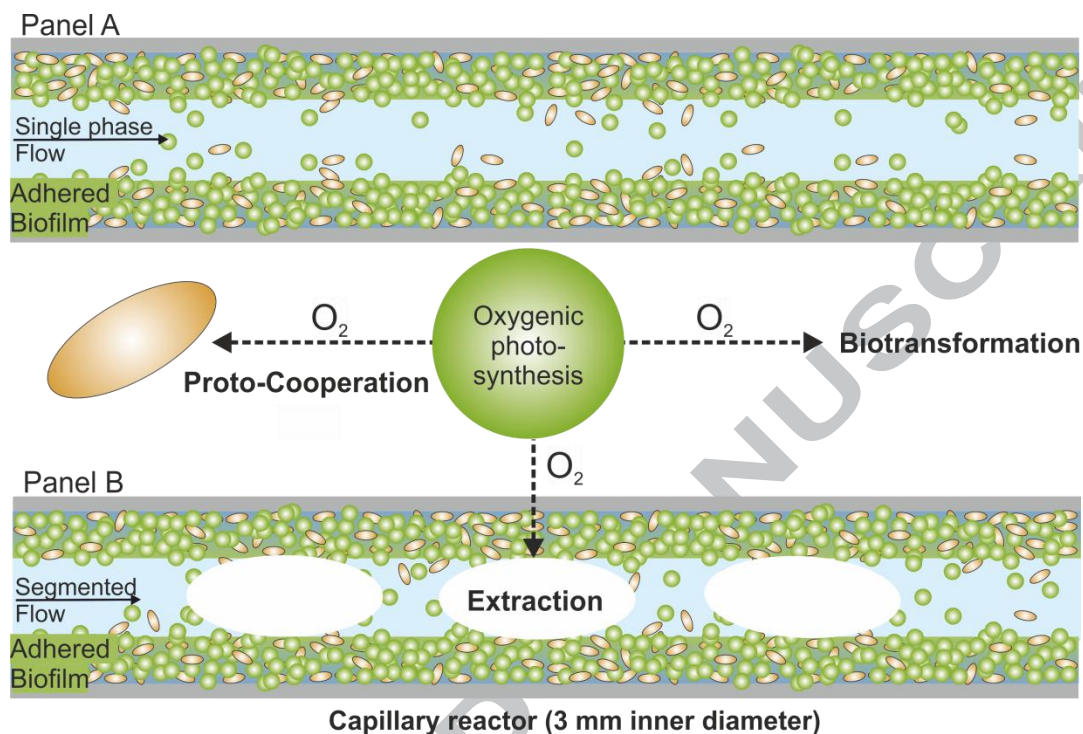
Figures

Fig. 1 Dual-species HCD biofilm cultivation in a capillary reactor. A photoautotrophic strain (here *Synechocystis* sp. PCC 6803; green cell) producing O_2 is cultivated together with a heterotrophic microbe (here *P. taiwanensis* VLB120; brown cell) as a biofilm in a capillary reactor. Growth medium is continuously running through the capillary. The system can be operated either under mere aqueous flow (Panel A) or under segmented flow (Panel B), where air segments are pumped through the system. For HCD cultivation it is crucial, that the oxygen concentration in the system is low. This oxygen removal can be achieved either via respiration using proto-cooperation, the introduction of an O_2 dependent reaction, or by extraction of O_2 into air segments flowing through the capillary reactor.
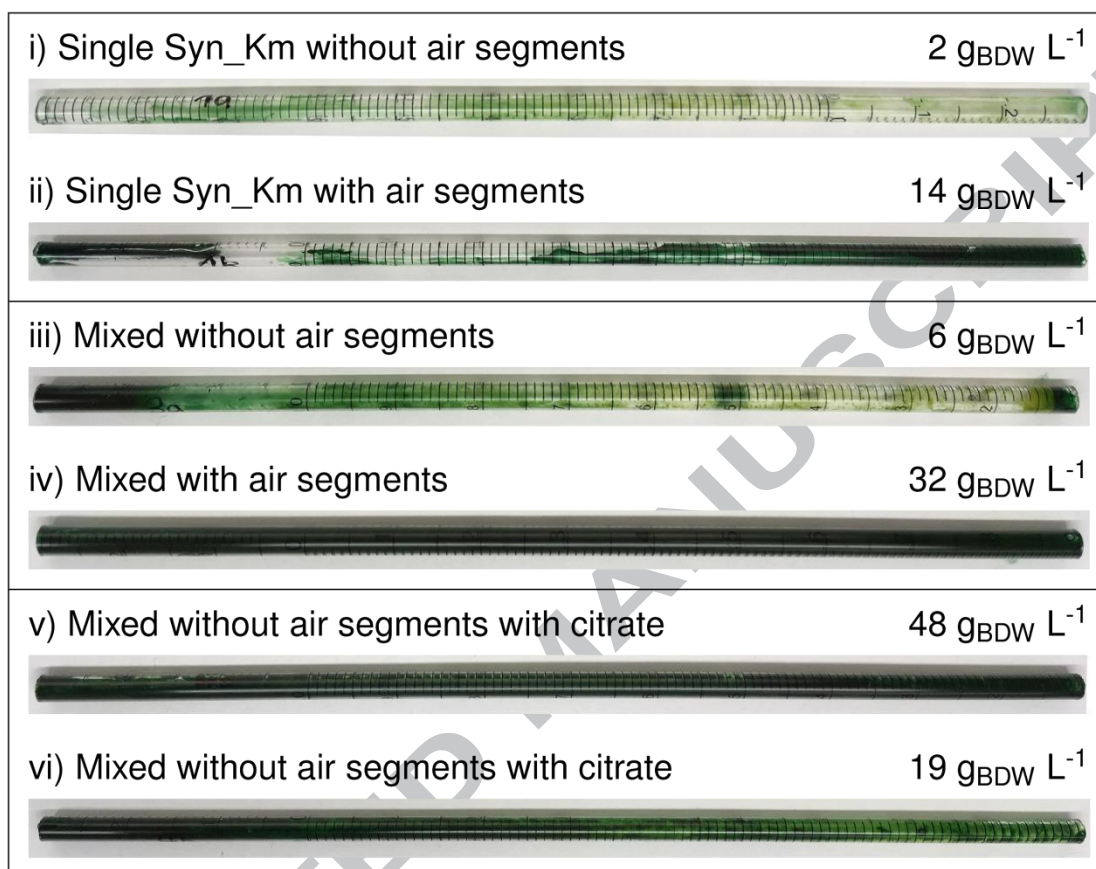
Fig. 2 Images of the biofilm capillary reactors 5 weeks after inoculation. i) and ii) depict monoseptic biofilm cultures of *Synechocystis* sp. PCC 6803 (pAH032) (Syn_Km) without and with air segments, respectively. Dual species biofilm cultures of Syn_Km and *P. taiwanensis* VLB120 (pAH032) were inoculated at a ratio of 1:1 and operated iii) without and iv) with air segments. v) and vi) correspond to iii) and iv) with citrate in the aqueous medium feed. Final biomass concentrations are given on the right of the respective image. Aqueous medium was fed at a rate of 52 µL min^{-1}. For segmented flow, a gaseous air phase was additionally fed at the same rate. BDW, biomass dry weight.
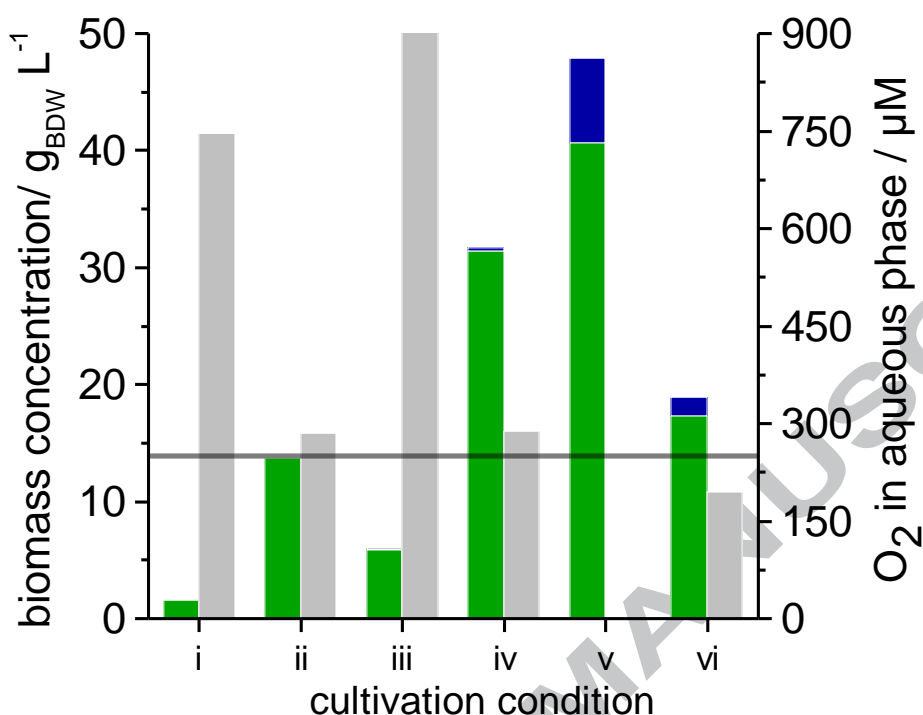
Fig. 3 O_2 and final biomass concentrations of single- and dual-species biofilms grown in capillary biofilm reactors after 5 weeks of cultivation. Grey bars refer to the aqueous O_2 concentrations measured at reactor outlets (left axis). Filled bars refer to the biomass dry weight per capillary volume ($g_{BDW}L^{-1}$, right axis). The green part of the filled bars corresponds to the *Synechocystis* sp. fraction and the blue one to the respective *Pseudomonas* fraction. The black line indicates O_2 saturation under ambient conditions (1 atm; 25 °C). Indices given on the x-axis refer to the different cultivation settings as defined in the legend of Figure 2. BDW, biomass dry weight
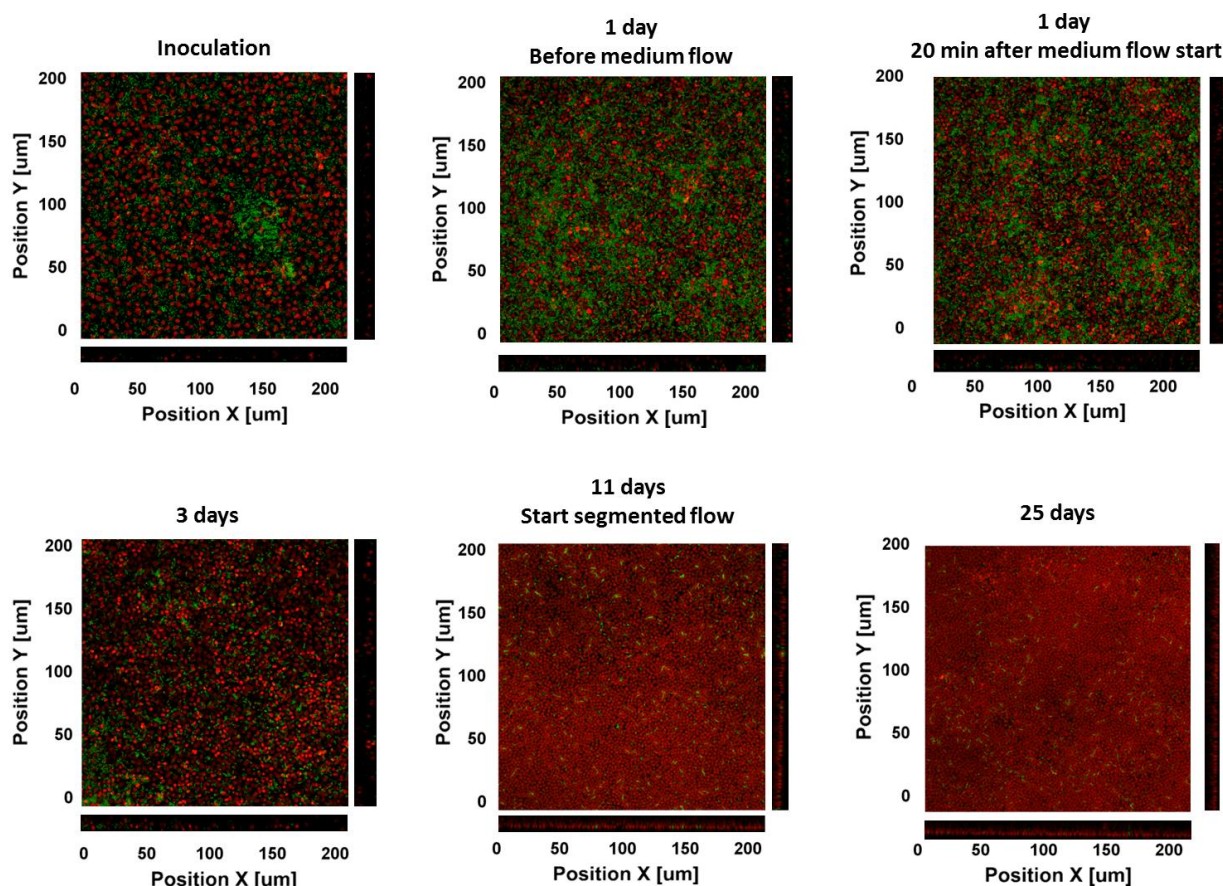
Fig. 4 3D Reconstruction of CLSM images showing the growth of a dual-species mixed trophies biofilm under aqueous as well as aqueous-air segmented flow conditions. Green and red cells correspond to *P. taiwanensis* VLB120 with a green fluorescent protein encoding *egfp* gene integrated into its genome and *Synechocystis* sp. PCC 6803 with its chlorophyll an autofluorescence, respectively (eGFP: 488 nm laser line, 4.0% laser intensity, 620 detector gain, chlorophyll autofluorescence: 633 nm laser line, 1.0% laser intensity, 500 detector gain). The biofilm was cultivated in YBG11 medium at 22 °C. All images were reconstructed and analyzed using IMARIS (8.2.0). Quantitative data are given in Heuschkel et al., 2019.
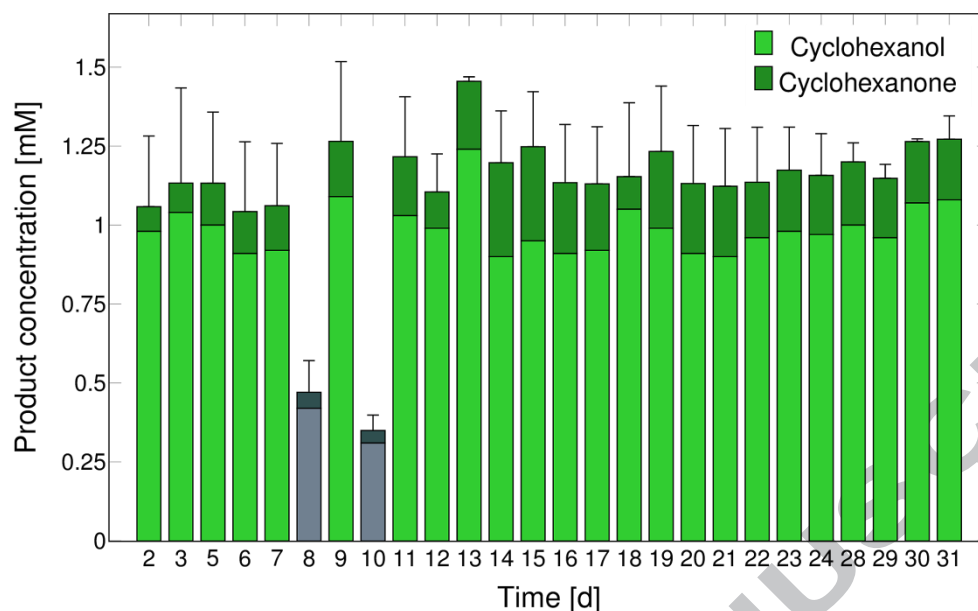
Fig. 5 Biocatalytic cyclohexane oxyfunctionalization utilizing recombinant

Synechechocystis sp. PCC 6803 (pAH050) and *P. taiwanensis* VLB 120 (pAH050) in a

dual-species mixed trophies biofilm. Biotransformation (started day 0 in Fig. 5) was

initiated after 5 weeks of biofilm cultivation. Experiments have been conducted at RT and

50 µE m^{-2} s^{-1} providing organic carbon free YBG11 medium and air segments at a flow rate

of 52 µL min^{-1}. The light was switched off during days 8 and 10 for 24 hours, respectively.

Green and gray bars represent product formation under light and dark conditions,

respectively. Light and dark colors refer to the formation of cyclohexanol and

cyclohexanone, respectively. (Further information are given in Heuschkel et al., 2019).

Highlights:

o   Mixed-trophies biofilm for the cultivation of high cell density photobiocatalysts

o O_2 toxification was overcome by respiration, extraction, and biotransformation

o   Mixed-trophies biofilms produce 3.76 g m^{-2} day^{-1} cyclohexanol for over a month

o   Cyclohexane conversion of 98% and KA oil selectivity of 100% was obtained